

UNCLASSIFIED

Approved for public release; distribution is unlimited

(U) Frequency-Wavenumber (F-K) Processing for Infrasound Distributed Arrays

October 2012

R. Daniel Costley¹, Wm. Garth Frazier², Kevin Dillion³, Jennifer Picucci¹, Jay Williams³,
and Mihan H. McKenna¹

¹U.S. Army Engineer Research and Development Center
3909 Hall Ferry Road, Vicksburg MS 39180

²National Center for Physical Acoustics, University of Mississippi
University MS USA 38677

³Miltec, Corp., Ducommun Incorporated
9 Industrial Park Drive, Oxford MS 38655

ABSTRACT

Microbarometers have conventionally been used to detect infrasound. Pipe arrays, used in conjunction with microbarometers, provide noise reduction by averaging wind noise over a large aperture. In recent years, distributed arrays have been used for the same effect. In addition to reducing wind noise via spatial averaging, these arrays have the ability to process the individual signals from each sensor to estimate the Direction of Travel (DOT) of acoustic signals. This is especially true for infrasound and low-frequency acoustic sources of tactical interest in the 1 to 100 Hz range. The work described herein discusses the application of a frequency-wave number (F-K) signal processing technique to signals from rectangular infrasound arrays for detection and estimation of DOT of infrasound. Arrays of 100 sensors were arranged in square configurations with the sensor spacing of 2 m. Wind noise data were collected at one site. Synthetic infrasound signals were superposed on top of the wind noise to determine the accuracy and sensitivity of the technique with respect to signal-to-noise ratio. The technique was then applied to an impulsive event recorded at a different site. Preliminary results demonstrated the feasibility of this approach.

Permission to publish was granted by Director, Geotechnical and Structures Laboratory.

UNCLASSIFIED

Report Documentation Page				Form Approved OMB No. 0704-0188	
Public reporting burden for the collection of information is estimated to average 1 hour per response, including the time for reviewing instructions, searching existing data sources, gathering and maintaining the data needed, and completing and reviewing the collection of information. Send comments regarding this burden estimate or any other aspect of this collection of information, including suggestions for reducing this burden, to Washington Headquarters Services, Directorate for Information Operations and Reports, 1215 Jefferson Davis Highway, Suite 1204, Arlington VA 22202-4302. Respondents should be aware that notwithstanding any other provision of law, no person shall be subject to a penalty for failing to comply with a collection of information if it does not display a currently valid OMB control number.					
1. REPORT DATE OCT 2012		2. REPORT TYPE N/A		3. DATES COVERED -	
4. TITLE AND SUBTITLE Frequency-Wavenumber (F-K) Processing for Infrasound Distributed Arrays				5a. CONTRACT NUMBER	
				5b. GRANT NUMBER	
				5c. PROGRAM ELEMENT NUMBER	
6. AUTHOR(S)				5d. PROJECT NUMBER	
				5e. TASK NUMBER	
				5f. WORK UNIT NUMBER	
7. PERFORMING ORGANIZATION NAME(S) AND ADDRESS(ES) 1U.S. Army Engineer Research and Development Center 3909 Hall Ferry Road, Vicksburg MS 39180				8. PERFORMING ORGANIZATION REPORT NUMBER	
9. SPONSORING/MONITORING AGENCY NAME(S) AND ADDRESS(ES)				10. SPONSOR/MONITOR'S ACRONYM(S)	
				11. SPONSOR/MONITOR'S REPORT NUMBER(S)	
12. DISTRIBUTION/AVAILABILITY STATEMENT Approved for public release, distribution unlimited					
13. SUPPLEMENTARY NOTES See also ADM202976. 2012 Joint Meeting of the Military Sensing Symposia (MSS) held in Washington, DC on October 22-25, 2012.					
14. ABSTRACT Microbarometers have conventionally been used to detect infrasound. Pipe arrays, used in conjunction with microbarometers, provide noise reduction by averaging wind noise over a large aperture. In recent years, distributed arrays have been used for the same effect. In addition to reducing wind noise via spatial averaging, these arrays have the ability to process the individual signals from each sensor to estimate the Direction of Travel (DOT) of acoustic signals. This is especially true for infrasound and low-frequency acoustic sources of tactical interest in the 1 to 100 Hz range. The work described herein discusses the application of a frequency-wave number (F-K) signal processing technique to signals from rectangular infrasound arrays for detection and estimation of DOT of infrasound. Arrays of 100 sensors were arranged in square configurations with the sensor spacing of 2 m. Wind noise data were collected at one site. Synthetic infrasound signals were superposed on top of the wind noise to determine the accuracy and sensitivity of the technique with respect to signal-to-noise ratio. The technique was then applied to an impulsive event recorded at a different site. Preliminary results demonstrated the feasibility of this approach.					
15. SUBJECT TERMS					
16. SECURITY CLASSIFICATION OF:			17. LIMITATION OF ABSTRACT SAR	18. NUMBER OF PAGES 10	19a. NAME OF RESPONSIBLE PERSON
a. REPORT unclassified	b. ABSTRACT unclassified	c. THIS PAGE unclassified			

1.0 Introduction

The use of distributed arrays for the detection and measurement of infrasound has become more common in recent years. On 5 September 2005 and 25 March and 21 July 2006, rockets were launched and detonated over the White Sands Missile Range for the purpose of creating infrasound.¹ Resulting infrasonic signals were detected by sensors that were deployed at various stations throughout the Southwest. A 96-element array was deployed at an infrasound station near Socorro, NM.¹ From the time dependence of the phase of the sound signal across the array, it was possible to determine the direction of the infrasound in the New Mexico rocket experiments, in addition to reducing wind noise.² This is especially true for sources of tactical interest, in the 1-100 Hz frequency range.

Arrays of point sensors were used previously in the study of wind noise. Bass showed that cross-correlation between pairs of microphones in a three-element array could be used to determine wind speed and direction.³ Shields conducted experiments with 28 sensors distributed over three orthogonal axes with a spacing of 0.61 m.⁴ He investigated the correlation in pressure fluctuations due to wind-noise as a function of distance measured in wavelengths of wind noise, after the wind noise was passed through a narrowband filter. This was performed in the downwind, crosswind, and vertical directions. Wilson *et al*, used a horizontal, planar array of 7 by 7 microphones to study wind-noise and distinguish it from sound.⁵ The spacing between neighboring microphones was 0.152 m. The sensor separations were smaller than the size of the turbulent eddies so that the wind-noise was “substantially correlated.” They used wavelet transform techniques to demonstrate the propagation of wind-noise (turbulent eddies) and sound across the microphone array.

The work described in this article is the application of frequency-wavenumber (F-K) processing to detect infrasonic signals and determine their direction of travel (DOT).⁶ The sensor spacing was over ten times than that of Wilson. At these spacings, one would expect the wind-noise to be correlated only at very low frequencies. In addition, the number of elements in the work describe here was about double, and the array aperture was almost 20 times as large. In addition, the acoustic signals of interest were lower in frequency in what is regarded as the tactical infrasound range. The array and the sensors are described in the first section, along with the signal processing technique. In order to assess the performance of the processing technique, synthetic infrasound signals were superposed on recorded wind-noise. The performance of the array, in terms of signal-to-noise ratio (SNR), is presented. The F-K technique is then used to process signals of an explosion recorded with the array.

2.0 Array Configuration and Process Description

A 10 by 10 planar, horizontal, sensor array was deployed for a month at Pinon Flat, California in order to compare its wind noise filtering capabilities to the standard IMS pipe array located there.² The rows were parallel to the North-South axis, and the columns were parallel to West-East, with the positive x axis pointing South and the positive y axis pointing East. The distances between adjacent rows and columns were 2 m, so that the total size of the array was 18 by 18 m. Wind noise collected by a row of sensors over a 5.12 sec interval is shown in Figure 1. The pressure at each sensor was acquired at a rate of 200 samples per second. In addition, an acoustic anemometer located at the center of the array measured wind speed and direction at a height of approximately one meter above the ground. The wind speed during the time indicated in Figure 1 varied from 3 to 5 m/s.

The sensors in the array are high-impedance, charge-generating devices and are described in more detail by Shields⁴. When used with the appropriate data acquisition system, they have a flat frequency response from 0.02 Hz to 100 Hz. As discussed by Shields, the response of the individual elements in the arrays were shown to reduce the power spectrum of the wind noise by a factor of $1/N^{1/2}$, where N is the number of sensors, for frequencies above where the sensor separation is greater than about $1/4$ the wind noise wavelength (average wind velocity/frequency).

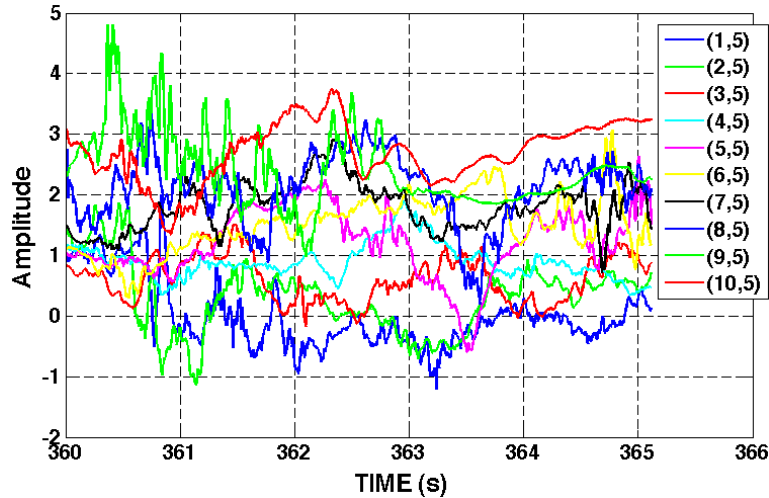


Figure 1. The traces represent 5.12 sec of wind noise recorded by a S-N row of sensors. The ordered pairs in the legend represent the position of the sensor in the array, with (1,5) being near the middle of the North most column and (10,5) being near the middle of the South most column.

2.1 Synthetic Infrasonic Signals

In order to simulate acoustic signals and to demonstrate the methodology, a simulated Gaussian-modulated sinusoidal pulse with a center frequency of 10 Hz was added to each signal in the array. The simulated signals that would have been recorded with the same row of sensors depicted in Figure 1 are plotted in Figure 2. The appropriate phase was added to the simulated signal recorded at each sensor to represent an acoustic signal with a direction of travel (DOT) of 30° and sound speed of $c = 340$ m/s.

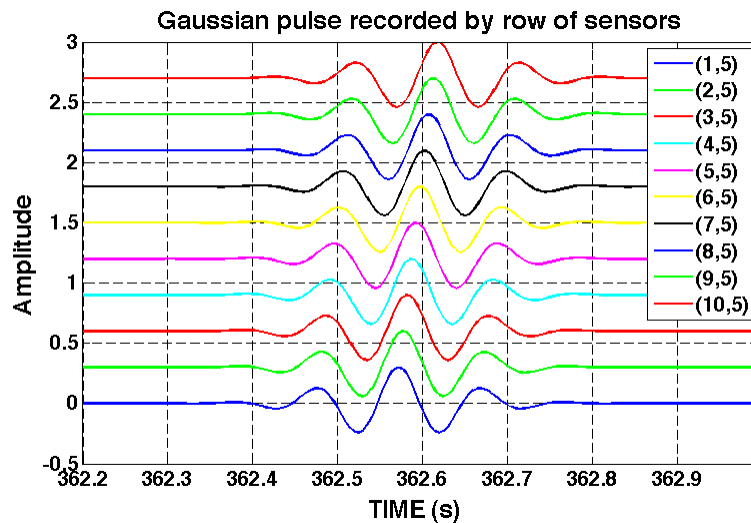


Figure 2. The traces represent the simulated Gaussian-modulated pulse hypothetically recorded by a S-N row of sensors, with delays to simulate propagation over the array.

Consider now a time harmonic acoustic wave traveling across the array that can be represented by the equation

$$p(x, y, t) = A * \cos(2\pi ft - k_0 x \cos \theta - k_0 y \sin \theta + \phi) \quad (1)$$

where A , f , t , and k_0 represent amplitude, frequency, time, and wave number, respectively. The angle θ represents the DOT with respect to South, and ϕ is an arbitrary phase term. (The difference between DOT and direction of arrival (DOA) is 180° .) The x and y components of the wave number are given by $k_x = k_0 \cos \theta$ and $k_y = k_0 \sin \theta$, where $k^2 = k_x^2 + k_y^2$, $k = 2\pi/\lambda$, and λ is the wavelength. In this formulation, the wavenumber is in terms of wavelengths per radian. The wavenumber can also be represented as $v = k_0/(2\pi) = 1/\lambda = f/c$, where c represents the speed of sound in air. In this case, $v_x = k_x/(2\pi)$ and $v_y = k_y/(2\pi)$ are the x and y components of the wave number in terms of wavelengths per unit distance.

When a sound of a given frequency passes over the array, the magnitude of the 2-D Fast-Fourier Transform (FFT) corresponding to that frequency will have a maximum that corresponds to the prevailing wavenumbers of the disturbance. Both the speed of the disturbance and the direction of travel can be determined from the wavenumbers using the above relations.

The F-K processing technique is implemented by first applying an FFT to the temporal signals from each sensor. The signals had a window length of 1024 samples, 5.12 s, and were zero padded to 4096 samples. The complex values were stored in a 10 by 10 by 4096 array corresponding to the dimensions x , y , and f , where f represents frequency. The spatial dimensions were zero padded to 128 by 128 samples. A 2-D FFT was applied along the 10 by 10 dimensions of the array, corresponding to the spatial directions, for a specific value of frequency. The magnitude of the 2-D FFT is referred to as the wavenumber spectrum corresponding to the specific frequency bin.

The phase-delayed Gaussian-modulated sinusoidal pulse described above, without added wind noise, was processed using the procedure described in the preceding paragraph to calculate the wavenumber spectrum for the 10 Hz frequency bin. The magnitude of this spectrum is plotted in Figure 3(a), with v_x and v_y represented along the horizontal and vertical axes, respectively. The global maximum is clearly evident. The speed of sound and direction of travel are determined from the values of v_x and v_y at this maximum. In this case, the speed of sound and the direction of travel turn out to be 317.8 m/s and 29.7° . One might expect the results to be closer to the values input to the simulated waveform, since the simulated signal contained no noise. It turns out that the error was due to discretization in both the temporal and spatial domains. The results of different zero padding schemes, listed in Table 1, show that the wavenumber resolution changes with zero padding. Thus, the x and y components of wavenumber are quantized, depending on the amount of zero padding, which means that the values of sound speed and direction are also quantized. The spatial padding affects the x and y components of the wavenumber differently so that the improvement is not always monotonic with zero padding. The analytical results listed in Table 1 correspond to wavenumber components and frequency calculated directly from the algebraic relations for sound speed and direction, listed above. The zero padding of the temporal signals was not changed in this example; however, that would also affect the results. The signals were sampled in both the temporal and spatial domains with rectangular, or boxcar, windows. Other window functions, such as Hamming, might reduce the discretization error. At the very least, it would reduce the amplitude of the side lobes seen in Figure 3(a).

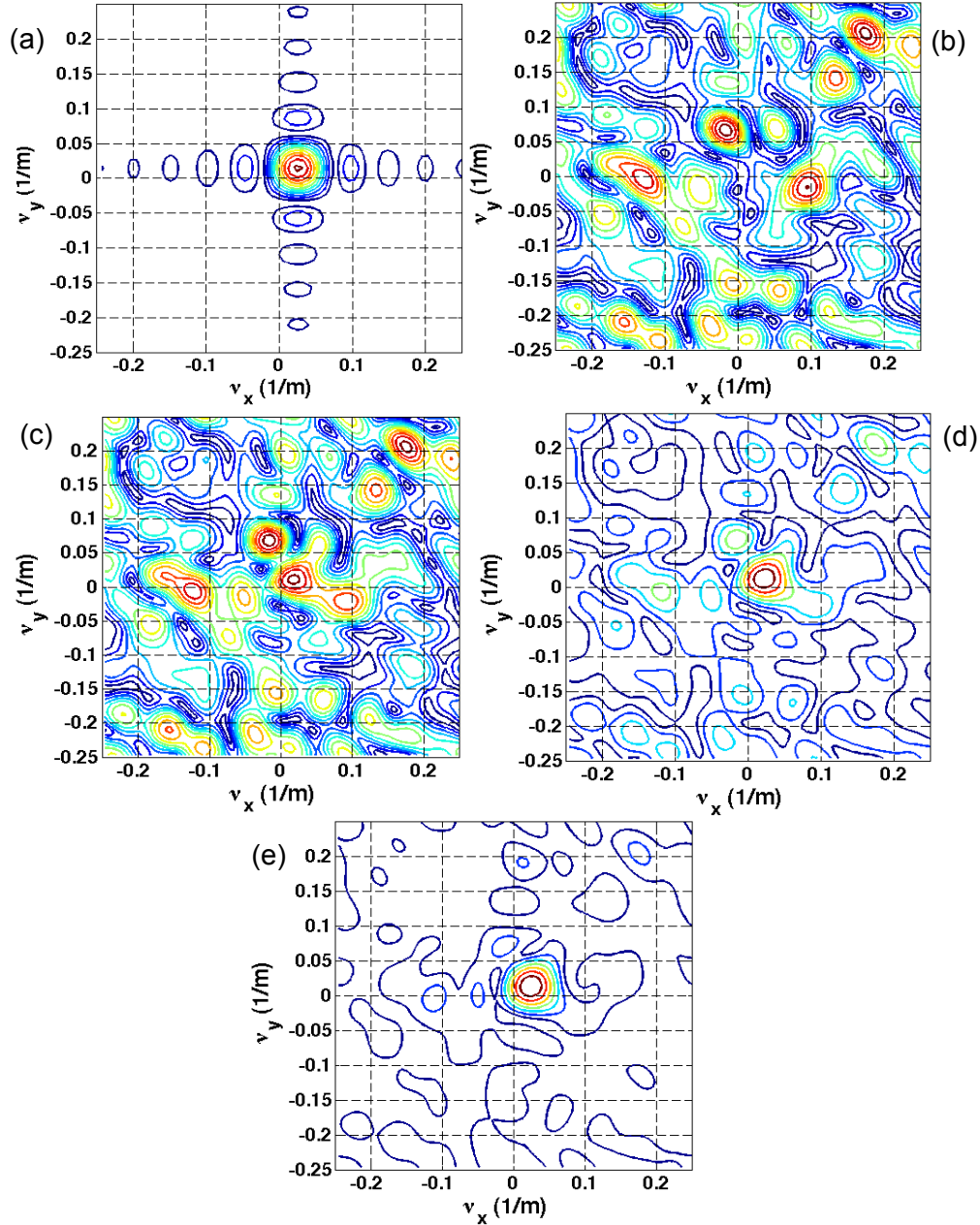


Figure 3. Wavenumber spectra of the Gaussian pulse traveling over the infrasound array corresponding to various SNR.

2.2 Wind-noise Processed with Synthetic Infrasonic Signals

The simulated Gaussian-modulated sinusoidal pulse was added to wind noise signals collected at Pinion Flats and processed as described above. The amplitude of the pulse was varied to determine the performance of the process as a function of signal-to-noise ratio (SNR). The SNR was determined as the ratio magnitudes of the pressure spectra of the pure signal and pure wind noise in the 10 Hz bin. These results are plotted in Figures 3(b-e). The data from Pinion flats consisted of a record of 900 sec duration. These spectra were obtained from the 5.12 sec interval starting at 360 sec. The wavenumber spectrum for a single frequency bin contains $128^2 = 16,384$ complex values.

The wavenumber spectrum in Figure 3(b) corresponds to pure wind noise, *i.e.*, $\text{SNR} = 0$. The spectrum shows no distinguishing feature, with several local maxima and minima. The spectrum in Figure 3(c), which corresponds to $\text{SNR} = 0.31$, has many of the same features as the pure noise spectrum. However, a small maximum appears near the origin in the top-right quadrant. The SNR is increased to 0.51 for the spectrum in Figure 3(d). The peak near the origin has grown in magnitude with respect to the other maxima. The other maxima have the same magnitude as before, but they appear smaller because the same number of contours is used to span a greater difference in magnitudes. Figure 3(e) represents the spectrum when $\text{SNR} = 1.0$. The peak corresponding to the acoustic pulse dominates the spectrum.

The SNR was varied from approximately 0.02 to 2.5 by changing the amplitude of the pulse superposed on the wind noise. Wavenumber spectra from each of these cases were used to determine the speed of sound and the DOT. The results are plotted in Figure 4. The plots show that the acoustic pulse is detected when the $\text{SNR} > 0.3$. The error generally decreases as SNR increases up to $\text{SNR} \approx 0.7$. However, the error in DOT is the lowest when $0.3 < \text{SNR} < 0.5$. This is probably because discretization error affects v_x and v_y differently, as mentioned above. The actual values in the plots correspond to the analytical values of $\text{DOT} = 30^\circ$ and $c = 340 \text{ m/s}$.

Table 1. Location of maximum of wavenumber spectra changes slightly with spatial zero padding.

zero pad	$\Delta v \text{ (m}^{-1}\text{)}$	$v_x \text{ (m}^{-1}\text{)}$	$v_y \text{ (m}^{-1}\text{)}$	$\theta \text{ (}^\circ\text{)}$	$c \text{ (m/s)}$
analytical		0.02547	0.01471	30	340
64 pts	0.0078	0.02344	0.01563	33.7	355.4
128 pts	0.0039	0.02734	0.01563	29.7	317.8
256 pts	0.0020	0.02539	0.01563	31.6	335.8

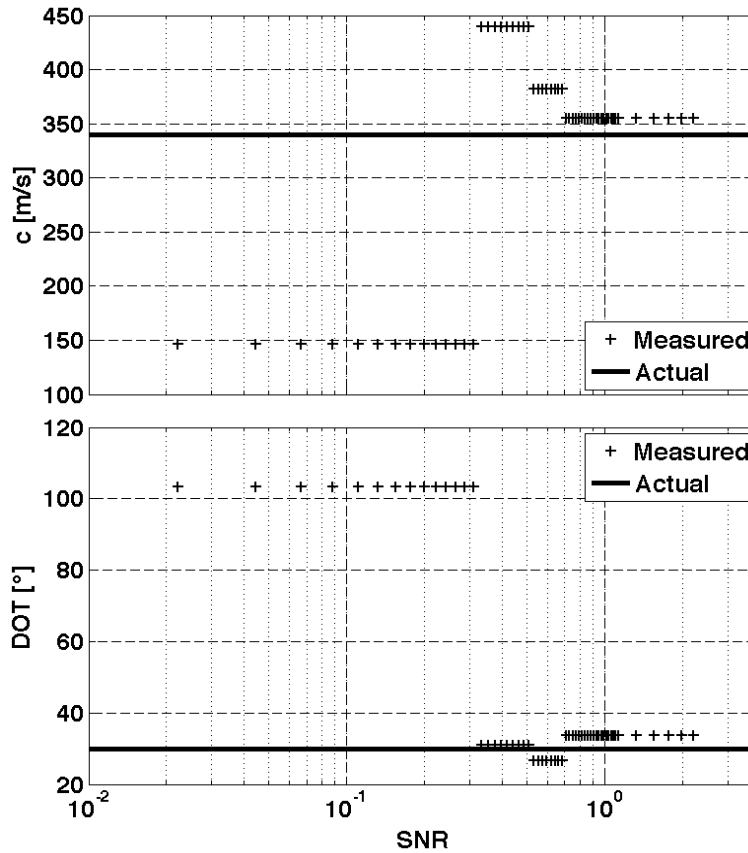


Figure 4. Top: Speed of sound is plotted as a function of SNR; Bottom: Direction of -Travel is plotted as a function of SNR. Plus signs represent 3-D FFT results from simulated signal superposed on wind noise. The horizontal solid lines represent the input parameters to the simulated Gaussian-modulate sinusoidal signal: $c = 340$ m/s and $\text{DOT} = 30^\circ$.

3.0 Recorded Explosive Event

The same array was deployed at another location where an explosive event of unknown nature was recorded. The signals recorded by a row of sensors are plotted in Figure 5. The bottom plot in Figure 5 shows wind noise collected with the same row of sensors. The wind was calmer than from the Pinion Flats recording. An acoustic anemometer measured wind speeds between 0.5 and 2.0 m/s.

The wavenumber spectra technique was applied to these data with encouraging results. Figure 6(a) shows a wavenumber spectrum for the 10 Hz bin during a period of only wind noise. The spectrum is noisy, but there is a maximum near the origin. It turns out that the distance of the peak from the origin, in wavenumber coordinates, along with the frequency determines the speed of propagation. In this case, the speed associated with this maximum is 1803 m/s. This could represent sound traveling at near normal incidence to the ground, such as from an aircraft flying overhead; however, the magnitude at the maximum (8.6) is very low.

Figure 6(b) shows the wavenumber spectrum from the 10 Hz bin associated with an explosion recorded by the array. The maximum is located at $v_x = 0.0273 \text{ m}^{-1}$ and $v_y = -0.00391 \text{ m}^{-1}$ and has a magnitude of 125. The speed of sound and DOT associated with these wavenumber coordinates are 361 m/s and -8.1° with respect to array coordinates (DOT in SSW direction). An independent beam-forming technique estimated the DOT to be 0° to -5° , which is reasonable agreement. This corresponds to a DOA of 8.1° with respect to North, the general direction of the location of the explosion. For more confirmation, the same procedure was used to construct a wavenumber spectrum for the 13 Hz bin, which is plotted in Figure 6(c). The results from this spectrum are $c = 361 \text{ m/s}$ and $\text{DOT} = -12.5^\circ$.

Although not shown, it was observed that the magnitudes of the wavenumber spectra were smaller than those from the Pinion Flat spectra. One reason for this is that the intervals were smaller, 512 points rather than 1024 points (2.56 s vs. 5.12 s). Another reason is that the wind speed was significantly less, 1 to 2 m/s, rather than 3 to 5 m/s at Pinion Flats.

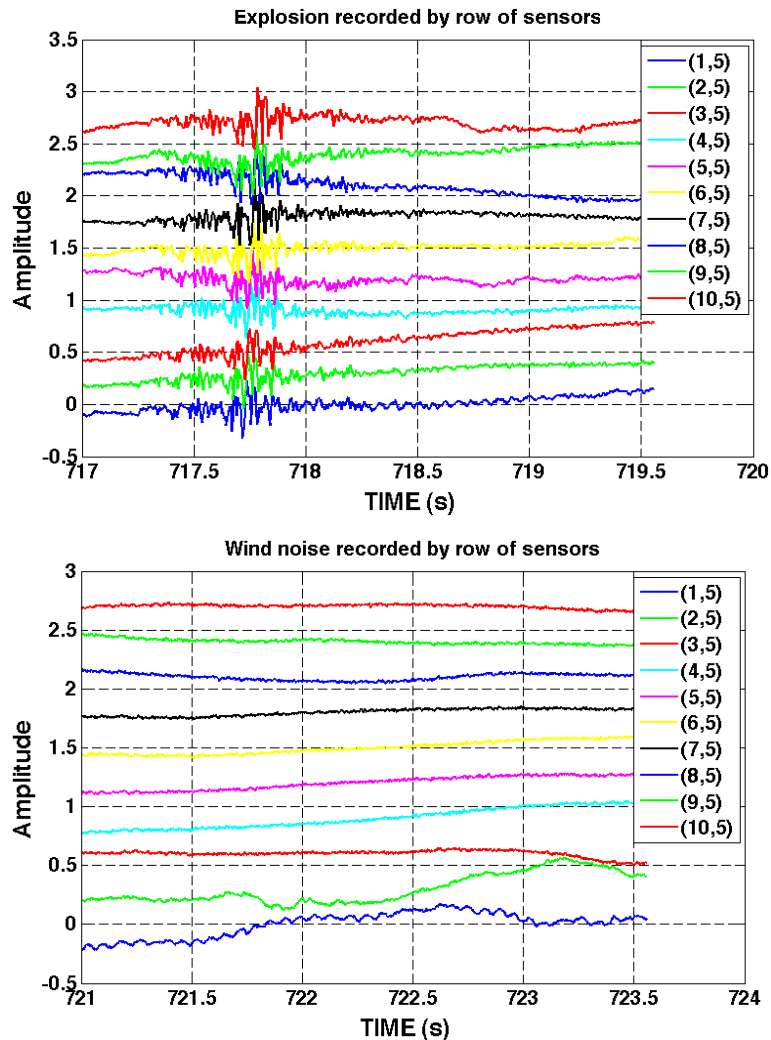


Figure 5. Top: An explosion recorded with a N-S row of sensors. Bottom: Wind-noise recorded with a N-S row of sensors.

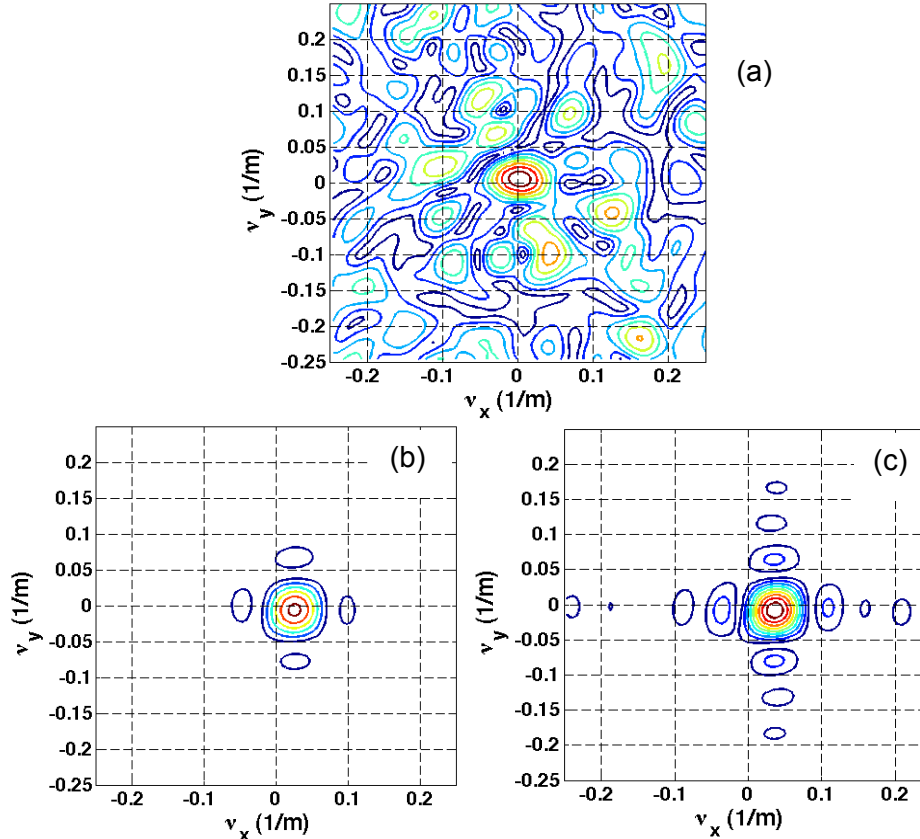


Figure 6. Wavenumber spectra from data collected with infrasound array: (a) wind-noise; (b) signal from explosive event in frequency bin centered at 10 Hz; and (c) adjacent frequency bin centered at 13 Hz.

4.0 Summary and Conclusion

A technique for processing evenly distributed arrays of infrasound sensors was presented. The performance of the technique was evaluated by superposing simulated signals on recorded wind noise. The results show that infrasound can be detected at SNR of 0.3 and that accuracy improves as SNR increases. The technique was then applied to a recorded explosion. The wave speed estimated with this technique was about 20 m/s greater than the text book value. This discrepancy represents an error of about 6%. However, it could indicate that the sound is not traveling parallel to the ground. An independent estimate of the DOT was approximately within 5° of the DOT determined with the F-K technique.

Future work will include the development of a statistical, adaptive threshold detector. Histograms of the magnitudes of the wavenumber spectra in the absence of an acoustic signal (not shown) indicate that they can be fit to a Gamma probability distribution function. These can be used to set thresholds based on an acceptable false alarm rate, which will change with wind noise levels.

Sensor spacing and array aperture will affect the effective bandwidth of the array. It was shown by trial and error that the current array was effective down to frequencies of approximately 4 Hz. Below that, the DOT could not be determined accurately. Increasing sensor spacing and array aperture can reduce the lower frequency limit.

UNCLASSIFIED

Such a large array has limited tactical value, unless it was to be used as part of a permanent installation. It would be interesting to investigate array configurations with fewer sensors and different configurations. A simple candidate would be two linear arrays of 10 elements each deployed perpendicular to each other. A 2-D FFT, one in the spatial dimension and the other temporal, should reveal the frequency-wavenumber spectrum of an acoustic wave traveling across the array. If the wave were traveling at an angle θ with respect to the array, the trace velocity across the array would be $c/\cos(\theta)$. The trace velocity corresponding to the perpendicular array would be $c/\sin(\theta)$. Thus, from the 2 FFTs, one should be able to determine the direction, wavelength and frequency of the acoustic signal. In that the two linear arrays would have fewer sensors than the larger 100-element array, one would expect that they would be able to detect signals only at higher SNRs. This would need to be investigated.

Also, both the linear arrays and the rectangular array will have directivity patterns that are not circular. In other words, they will detect in some directions better than they will at others. A circular array would have a circular directivity pattern. However, another processing scheme would have to be used to exploit this geometry. Perhaps a digital Hankel transform would serve this purpose.

In order for this approach to be useful, the processing will have to be performed in real-time. However, as mentioned earlier, the temporal signals were zero padded to 4096 samples, and the spatial signals were padded to 128 by 128 samples. Computational efficiency will require that the signals be zero padded with fewer points. In addition, more efficient algorithms will need to be developed or found. Using arrays with fewer array elements will make for faster processing, although accuracy and resolution may suffer.

In conclusion, arrays of evenly distributed infrasound sensors can be useful for accurately and precisely detecting infrasound and for determining DOT. The speed of travel of the disturbance is also determined, and this can be used as a criterion for discriminating sound from noise. Arrays with limited numbers of sensors could potentially be used in tactical situations where arrays with large numbers of elements would not be practical.

5.0 Acknowledgements

The U.S. Army Space and Missile Defense Command supported the data collection and the initial array processing work. Recent work was supported by the U.S. Army Engineer Research and Development Center. Permission to publish was granted by Director, Geotechnical and Structures Laboratory.

6.0 References

1. E.T. Herrin, P.W. Golden, H.E. Bass, D.E. Norris, B. Andre, C. de Groot-Hedlin, R.L. Woodward, K.T. Walker, D.P. Drop, C.A. Szuberla, M.A.H. Hedlin, R. W. Whitaker, M.A. Garces, F. D. Shields, "High-Altitude Infrasound Calibration Experiments," *Acoustics Today*, **4**(2), 9-17 (2008).
2. Dillion, K., Howard, W., Shields, F.D., "Advances in distributed arrays for detection of infrasound," *J. Acoust. Soc. Am.*, **122**(5) 2960 (2007).
3. H.E. Bass, R. Raspet, and J.O. Messer, "Experimental determination of wind speed and direction using a three microphone array," *J. Acoust. Soc. Am.* **97**(1), 695-696 (1995).
4. F. Douglas Shields, "Low-frequency wind noise correlation in microphone arrays," *J. Acoust. Soc. Am.*, **117**(6), 3489-3496 (2005).
5. Wilson, D.K., Greenfield, R.J., and White, M.J., "Spatial structure of low-frequency wind noise," *J. Acoust. Soc. Am.* **122**(6), EL223-EL228 (2007).
6. Costley, R.D., Frazier, W.G., and Dillion, K.D., "Array processing for direction of arrival of infrasound," *J. Acoust. Soc. Am.*, **129**(4) 2443 (2011).